

Probing the thermal history of the Intergalactic Medium with Ly α absorption lines

Martin G. Haehnelt¹ and Matthias Steinmetz^{1,2}

¹ *Max-Planck-Institut für Astrophysik, Postfach 1523, 85740 Garching, Germany*

² *Steward Observatory, University of Arizona, Tucson, AZ 85721, USA*

28 August 2018

ABSTRACT

The Doppler parameter distribution of Ly α absorption is calculated for a set of different reionization histories. The differences in temperature between different reionization histories are as large as a factor three to four depending on the spectrum of the ionizing sources and the redshift of helium reionization. These temperature differences result in observable differences in the Doppler parameter distribution. Best agreement with the observed Doppler parameter distribution between redshift two and four is found if hydrogen and helium are reionized simultaneously at or before redshift five with a quasar-like spectrum.

Key words: cosmology: theory, observation — intergalactic medium — quasars: absorption lines

1 INTRODUCTION

The physical conditions of the Intergalactic Medium (IGM) have been under discussion ever since its existence was postulated. The absence of strong Ly α absorption in the spectra of high-redshift objects showed that any homogeneous IGM must be either highly ionized or extremely tenuous (Gunn & Peterson 1965, Bahcall & Salpeter 1965). Nevertheless the IGM density and temperature have been poorly constrained for many years. Both a hot collisionally ionized IGM heated by energy input due to supernovae and a warm intergalactic medium heated by photoionization have been discussed extensively in the literature. Recent progress in numerical simulations including the relevant gas physics suggests that the low column density Ly α forest is due mainly to density fluctuations of moderate amplitude in a warm photoionized phase of the IGM (Cen et al. 1994; Petitjean, Mückel & Kates 1995; Zhang, Anninos & Norman 1995; Hernquist et al. 1996; Miralda-Escudé et al. 1996; but see also Bi, Börner & Chu 1992 for early analytical predictions). The baryon content in this warm phase must be similar to that predicted by cosmic nucleosynthesis to produce the observed mean absorption in the spectra of high-redshift quasars. At redshifts larger than two most of all baryons are therefore probably in such a warm phase of the IGM and little room is left for an additional hot phase. (Rauch & Haehnelt 1995, Rauch et al. 1997, Weinberg et al. 1997). As pointed out by a number of authors the recombination time scale of the IGM becomes longer than the Hubble time at a redshift of about five. As a result, the temperature of the warm IGM has some memory for when and how it was (re-)ionized (Miralda-Escudé

& Rees 1994, Meiksin 1994, Hui & Gnedin 1997). We have used a set of hydrodynamical SPH simulations for different plausible reionization histories to demonstrate that these do indeed result in significant and observable differences in the thermal history of the IGM. In this letter we investigate the observable consequences on the Doppler parameter distribution of Ly α absorption lines and speculate on the possibility to discriminate between different reionization histories.

2 REIONIZATION AND THE THERMAL HISTORY OF A PHOTOIONIZED INTERGALACTIC MEDIUM

We have calculated the thermal history of an IGM of primordial composition within a cosmological context using SPH simulations performed with GRAPESPH (see Steinmetz 1996 for a detailed description of the numerical techniques and Rauch, Haehnelt & Steinmetz 1997 for a description of their absorption properties). The code includes the relevant cooling and heating processes and follows self-consistently the non-equilibrium evolution of the baryonic species (H, H⁺, He, He⁺, He⁺⁺, and e⁻). For the low-density regime relevant in this paper the thermal evolution of the IGM is rather simple (Miralda-Escudé & Rees 1994, Hui & Gnedin 1997, Steinmetz & Haehnelt 1997). The dominant heat input is due to ionization of hydrogen and helium while the main cooling processes are Compton cooling at $z \gtrsim 5$ and adiabatic cooling at lower redshift. At reionization the gas acquires an initial temperature

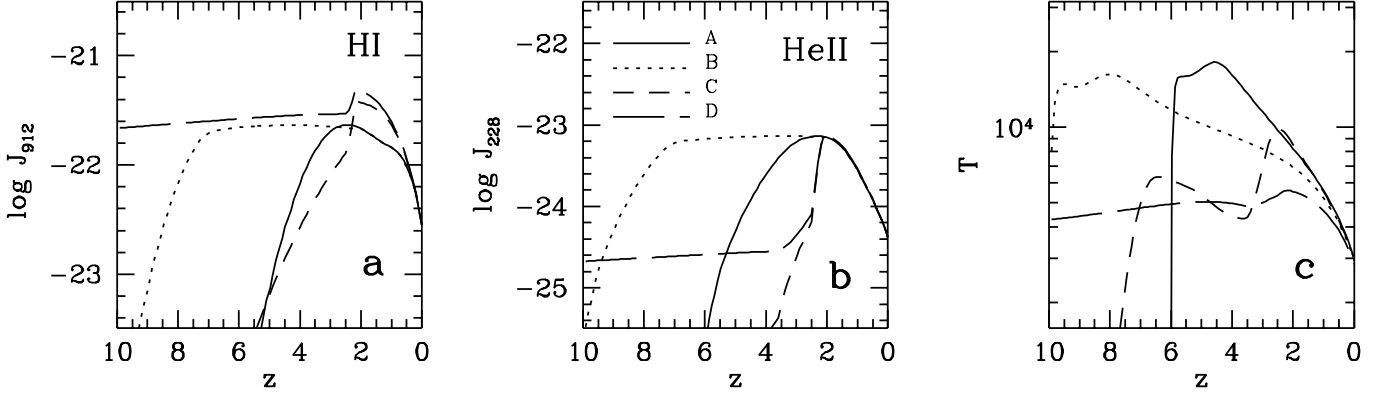


Figure 1. The left and middle panels show the absorption cross section-weighted specific intensity of the UV background at the HI and HeII ionization edges ($\int I_\nu \sigma \frac{d\nu}{\nu} / \int \sigma \frac{d\nu}{\nu}$) in units of $\text{erg cm}^{-2} \text{s}^{-1} \text{Hz}^{-1} \text{sr}^{-1}$ for four different models. The right panel shows the corresponding thermal history of the IGM at the mean density. For a description of models A–D see section 2.

$$\begin{aligned}
 T_i = & \frac{1}{3k_B} \int 4\pi I_\nu \left[(h\nu - h\nu_{\text{HI}}) \sigma_{\text{HI}} \right. \\
 & + (h\nu - h\nu_{\text{HeI}}) \sigma_{\text{HeI}} + (h\nu - h\nu_{\text{HeII}}) \sigma_{\text{HeII}} \left. \right] \frac{d\nu}{h\nu} \\
 & / \int 4\pi I_\nu \left[\sigma_{\text{HI}} + \sigma_{\text{HeI}} + \sigma_{\text{HeII}} \right] \frac{d\nu}{h\nu},
 \end{aligned} \tag{1}$$

where ν_X and σ_X are ionization energies and ionization absorption cross sections and I_ν is the specific intensity of the ionizing background. Afterwards the gas cools adiabatically within a Hubble time to the (redshift dependent) equilibrium temperature where photo-heating balances adiabatic cooling. The temperature of the gas therefore depends on the spectrum of the ionizing source and on the redshift when reionization occurs.

We have investigated four different models to cover the uncertainty concerning the respective role of quasars and stars in the reionization of the Universe:

Model A: Ionizing background as proposed by Haardt & Madau (1996). The spectrum is a power-law with $\alpha=1.5$ processed by the intervening Ly α absorption.

Model B: Same as model A but the redshift evolution is stretched towards higher redshift (“Early QSO’s”).

Model C: Same as model A but the redshift evolution is compressed towards lower redshift (“Late QSO’s”). A stellar component is added to the UV background which reionizes hydrogen at redshift $z \sim 6$ with a soft spectrum (power law with $\alpha=5$).

Model D: Same as C but the stellar component reionizes hydrogen at redshift $z \sim 30$.

Figures 1a and 1b show the evolution of the UV back-

ground for the four scenarios at the HI and HeII ionization edges respectively. At redshift three the HI ionizing flux is 1 to $3 \times 10^{-22} \text{erg cm}^{-2} \text{s}^{-1} \text{Hz}^{-1}$, slightly lower than estimates from the proximity effect but consistent with the mean flux decrement in QSO absorption spectra (Bechtold 1994; Giallongo et al. 1996; Cooke, Espey & Carswell 1997; Rauch et al. 1997). Model A was chosen by Haardt & Madau to represent the UV background due to observed quasars. Model B mimics the existence of an as yet undetected population of quasar at redshifts beyond five. Models C and D address the possibility that the Haardt & Madau model overestimates the UV background due to quasars at redshifts larger than three. In the latter case the UV background would have to be dominated by a stellar contribution at these redshifts. Figure 1c shows the temperature evolution of the IGM for the mean density at a given redshift. There are striking differences in the thermal history between the models. In models A and B hydrogen and helium are reionized almost simultaneously with a rather hard AGN-like spectrum. This leads to an initial temperature of about $2 \times 10^4 \text{K}$. Thereafter the temperature approaches the redshift dependent equilibrium temperature. In scenario C and D the stellar component of the UV background is too soft to reionize helium at the same time as hydrogen. This results in an initial temperature of $7 \times 10^3 \text{K}$ immediately after reionization – significantly smaller than in model A and B. In Model C the late reionization of helium due to the QSO component of the UV background leads to a corresponding jump in the temperature while in model D Helium reionization occurs gradually before the QSO component of the UV background dominates. In the observationally relevant redshift range between five and three the difference in temperature between the different models is as large as a factor 3 to 4.

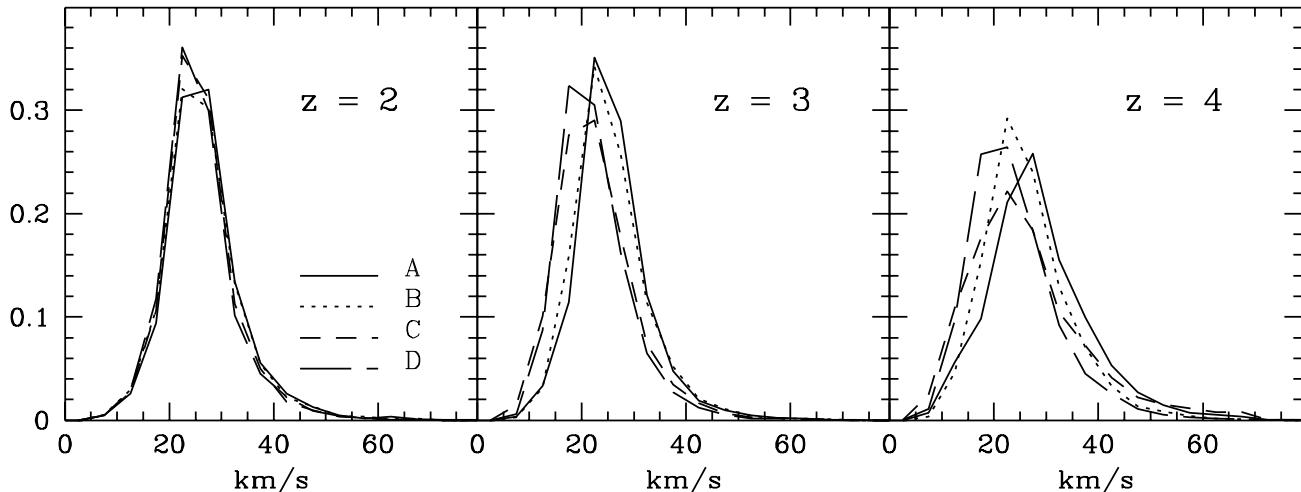


Figure 2. The distribution of the Doppler parameter obtained by profile fitting artificial spectra for models A–D for $z = 2, 3, 4$. The lines have column densities in the range $12.8 \leq N_{\text{HI}} \leq 16.0$.

3 SIMULATED AND OBSERVED DOPPLER PARAMETER

In Figure 2 we show the distribution of the Doppler parameter for the four scenarios at $z=2,3,4$. The Doppler parameters were obtained by fitting Voigt profiles to artificial spectra with the automatic line fitting program AUTOVP kindly provided by Romeel Davé (Davé et al. 1997). At redshift two the temperature in all four models is very similar and this is reflected by a nearly identical distribution of the Doppler parameters. At $z \geq 3$ the considerable differences in the temperature between the four models clearly carry over to the Doppler parameter distribution. In models C and D the distribution extends to smaller values of the Doppler parameter than in models A and B by about 5 km s^{-1} .

In the following we will present a preliminary comparison between observed and simulated Doppler parameter. It should, however, be kept in mind that that the primary aim of our paper is to demonstrate that there are observable differences between different reionization histories. There are a number of uncertainties in any comparison with the observed data. The observed Doppler parameter distributions we discuss have been obtained with different fit procedures. The spectrum of the UV background component due to star formation could be somewhat harder than the power law with $\alpha = 5$ which we have assumed. Furthermore our simulations do not include any feedback effects due to star formation and may therefore underestimate the fraction of the IGM in a hot collisionally ionized phase.

Figure 3 summarizes the comparison of observed and simulated Doppler parameter distribution at three different redshifts (Lu et al 1996, Kim et al 1997). The mean redshift and the column density range of the sample of lines identified with AUTOVP in the artificial spectra has been matched to those of the observed samples. At high redshift ($\langle z \rangle = 3.3, 3.7$)

there is good agreement between the observed and simulated Doppler parameter distribution in the case of models A and B. The only discrepancy is a modest high-velocity tail which is present in the observed data but not in the simulated distribution. Models C and D clearly disagree with the observed distribution. They show a considerable fraction of lines which are cooler than the lower cut-off of 15 km s^{-1} . At redshift 2.3 there is a significant discrepancy between simulated and observed distribution for all four models. The observed distribution shows a pronounced high-velocity tail which is not reproduced by any of the models. The existence of this high-velocity tail has been known for some time (e.g. Carswell et al. 1987) and appears to be real (Rauch et al. 1992, Press & Rybicki 1993).

4 DISCUSSION AND CONCLUSIONS

We have demonstrated that the range of plausible reionization and thermal histories for the universe result in observable differences in the Doppler parameter distribution of intermediate column density Ly α absorption lines at $z \sim 3$ to 5.

The observed Doppler parameter distribution at $z \gtrsim 3$ and the drop of the lower cut-off of the distribution from 20 to 15 km s^{-1} between redshift 2.3 and 3.7 is well reproduced if the universe is reionized with an AGN-like spectrum where hydrogen and helium are reionized simultaneously.

In the models where reionization occurs with a soft stellar spectrum roughly 10% of the lines at $z \sim 3.5$ have Doppler parameters between 10 and 15 km s^{-1} , well below the cut-off in the observed Doppler parameter distribution at this redshift (15 km s^{-1}). If the universe were to be reionized by a stellar component of the UV background, either

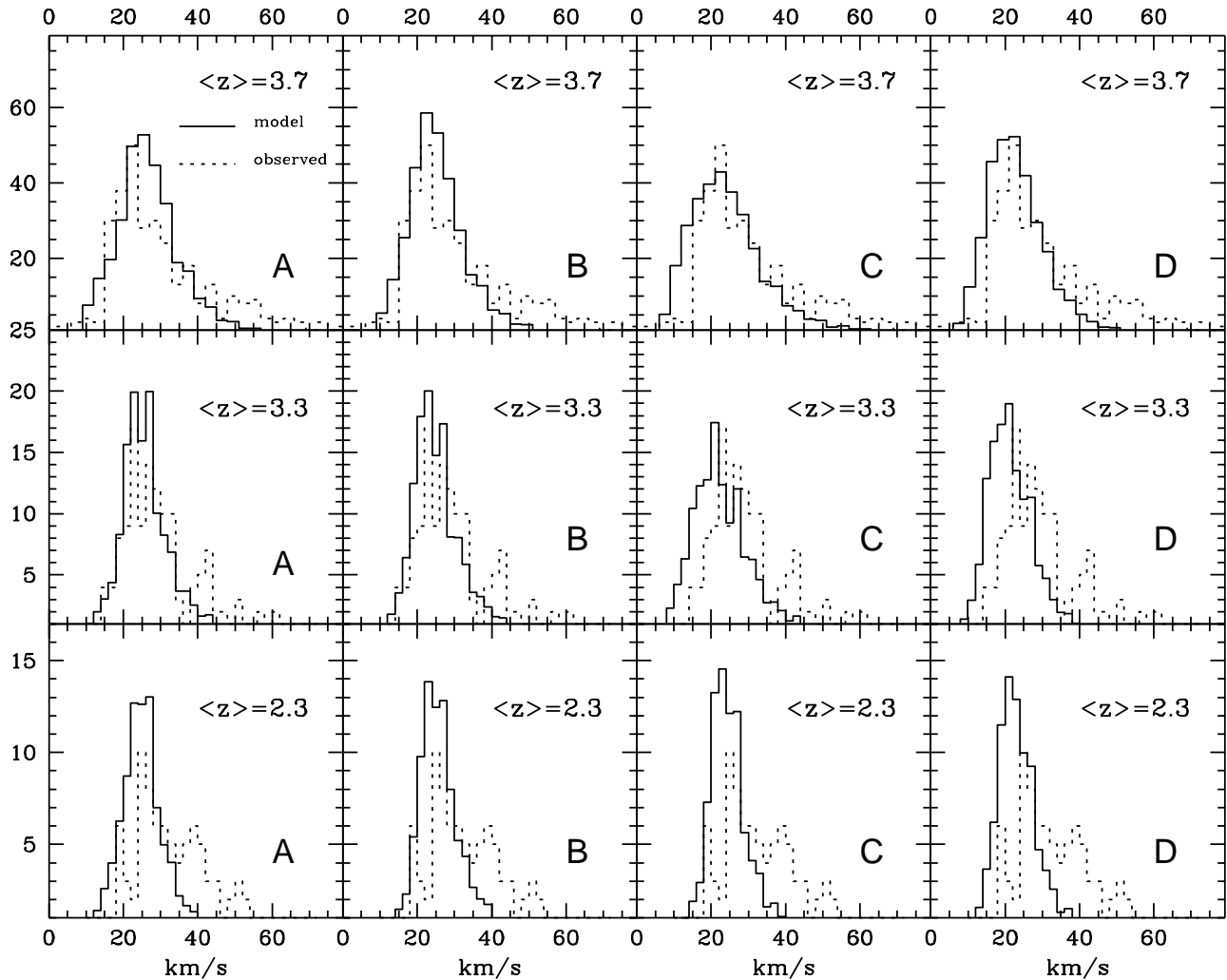


Figure 3. Observed (dashed line) and simulated (solid line) Doppler parameter distributions for models A–D (from left to right). The mean redshift of the samples is $\langle z \rangle = 2.3, 3.3, 3.7$. The observed data are taken from Lu et al. (1997) and Kim et al. (1997). The histograms of the simulated Doppler parameter are renormalized in each panel such that the area under the curves is the same as that of the observed distribution.

its spectrum would have to be hard enough to ionize helium and hydrogen at the same time, or the QSO contribution would have to become dominant before redshift four.

None of our models can explain the observed high-velocity tail of the observed low-redshift sample ($\langle z \rangle = 2.3$). About 15% of all observed lines at this redshift have Doppler parameters of 40 to 60 km s⁻¹ which would correspond to temperatures of 1 to 2 × 10⁵ K if the broadening were purely thermal. This is well above what can plausibly be reached by photoionization. This may indicate either, (i) that our simulations significantly underestimate the fraction of the IGM in a hot collisionally ionized phase because they do not include any feedback effects due to star formation or (ii) that there is a turbulent component to the broadening on scales below the resolution limit of the simulations which is more important at lower redshift.

Our results suggest that a larger and homogenous sam-

ple of lines, extending over a wider redshift range, will be an excellent tool to further constrain the reionization history.

ACKNOWLEDGMENTS

We thank Simon White for a careful reading of the manuscript and are grateful to Romeel Davé for providing the line-fitting software AUTOVP. Support by NATO grant CRG 950752 and the “Sonderforschungsbereich 375-95 für Astro-Teilchenphysik der Deutschen Forschungsgemeinschaft” is also gratefully acknowledged.

REFERENCES

- Bahcall J.N., Salpeter E.E 1965, ApJ ,142, 1677
 Bechthold, J. 1994, ApJS, 91,1
 Bi H.G., Börner G., Chu Y. 1992, A&A, 266, 1

- Carswell R.F., Webb J.K., Baldwin J.A., Atwood B., 1987, ApJ, 319, 709
- Cen R., Miralda-Escudé J., Ostriker J.P., Rauch M., 1994, ApJ, 437, L9
- Cooke A.J., Espey B., Carswell R.F., 1997, MNRAS, in press
- Davé R., Hernquist L., Weinberg D.H., Katz N., 1997, ApJ, in press, astro-ph/9609115
- Giallongo E., Cristiani S., D'Oderico S., Fontana A., Savaglio S., 1996, ApJ, 466, 46
- Gunn J.E., Peterson B.A., 1965, ApJ, 142, 1633
- Haardt F., Madau P., 1996, ApJ, 461, 20
- Hernquist L., Katz N., Weinberg D.H., Miralda-Escudé J., 1996, ApJ, 457, L51
- Hui L., Gnedin N.Y., 1997, MNRAS, in press
- Kim T.S., Hu E.M., Cowie L.L., Songaila A., 1997, AJ, in press, astro-ph/9704184
- Lu L., Sargent W.L.W., Womble D.S., Masahide T.-H., 1996, 472, 509
- Meiksin A., 1994, ApJ, 431, 109
- Miralda-Escudé, J., Cen, R., Ostriker, J.P., Rauch, M., 1996, ApJ, 471, 582
- Miralda-Escudé J., Rees M.J., 1994, MNRAS, 266, 343
- Petitjean, P., Mücke, J.P., Kates, R.E., 1995, A&A, 295, L9
- Press W.H., Rybicki G.B., 1993, ApJ, 418, 585
- Rauch M., Haehnelt M.G., 1995, MNRAS, 275, L76
- Rauch M., Haehnelt M.G., Steinmetz M., 1997, ApJ, 481, 601
- Rauch M., Miralda-Escudé J., Sargent W.L.W., Barlow T.A., Weinberg D.H., Hernquist H., Katz N., Cen R., Ostriker J.P. 1997, ApJ, submitted, astro-ph/9612245
- Rauch M., Carswell R.G., Chaffee F.H., Foltz C.B., Webb J.K., Weyman R.J. Bechthold J. Green R.G., 1992, ApJ, 390, 387
- Steinmetz M., 1996, MNRAS, 278, 1005
- Steinmetz M., Haehnelt M., 1997, in preparation
- Weinberg D.H., Miralda-Escudé J., Hernquist L., Katz, N., 1997, ApJ, submitted, astro-ph/9701012
- Zhang, Y., Anninos, P., Norman, M.L., 1995, ApJ, 453, L57